


The role of urea in neuronal degeneration and sensitization: An in vitro model of uremic neuropathy

Molecular Pain
Volume 15: 1–12
© The Author(s) 2019
Article reuse guidelines:
sagepub.com/journals-permissions
DOI: 10.1177/1744806919881038
journals.sagepub.com/home/mpx


U Anand^{1,2} , Y Korchev², and P Anand¹

Abstract

Background: Uremic neuropathy commonly affects patients with chronic kidney disease, with painful sensations in the feet, followed by numbness and weakness in the legs and hands. The symptoms usually resolve following kidney transplantation, but the mechanisms of uremic neuropathy and associated pain symptoms remain unknown. As blood urea levels are elevated in patients with chronic kidney disease, we examined the morphological and functional effects of clinically observed levels of urea on sensory neurons.

Methods: Rat dorsal root ganglion neurons were treated with 10 or 50 mmol/L urea for 48 h, fixed and immunostained for PGP9.5 and β III tubulin immunofluorescence. Neurons were also immunostained for TRPV1, TRPM8 and Gap43 expression, and the capsaicin sensitivity of urea- or vehicle-treated neurons was determined.

Results: Urea-treated neurons had degenerating neurites with diminished PGP9.5 immunofluorescence, and swollen, retracted growth cones. β III tubulin appeared clumped after urea treatment. After 48 hours urea treatment, neurite lengths were significantly reduced to $60 \pm 2.6\%$ (10 mmol/L, $**P < 0.01$), and to $56.2 \pm 3.3\%$ (50 mmol/L, $**P < 0.01$), compared with control neurons. Fewer neurons survived urea treatment, with $70.08 \pm 13.3\%$ remaining after 10 mmol/L ($*P < 0.05$) and $61.49 \pm 7.4\%$ after 50 mmol/L urea treatment ($**P < 0.01$), compared with controls. The proportion of neurons expressing TRPV1 was reduced after urea treatment, but not TRPM8 expressing neurons. In functional studies, treatment with urea resulted in dose-dependent neuronal sensitization. Capsaicin responses were significantly increased to $115.29 \pm 3.4\%$ (10 mmol/L, $**P < 0.01$) and $125.3 \pm 4.2\%$ (50 mmol/L, $**P < 0.01$), compared with controls. Sensitization due to urea was eliminated in the presence of the TRPV1 inhibitor SB705498, the mitogen-activated protein kinase kinase inhibitor PD98059, the PI3 kinase inhibitor LY294002 and the TRPM8 inhibitor N-(3-Aminopropyl)-2-[(3-methylphenyl)methoxy]-N-(2-thienylmethyl)benzamide (AMTB hydrochloride).

Conclusion: Neurite degeneration and sensitization are consistent with uremic neuropathy and provide a disease-relevant model to test new treatments.

Keywords

Chronic kidney disease, uraemia, neurodegeneration, sensitization, pain, neuropathy

Date Received: 26 March 2019; accepted: 3 September 2019

Introduction

Peripheral neuropathy affects 65% of patients with chronic kidney disease (CKD),^{1,2} presenting as a symmetrical length-dependent process with predominant sensory involvement.^{3–7} Lower limbs are affected to a greater extent than upper limbs, with pain and paraesthesia progressing over several months, and motor involvement, leading to weakness and compromised quality of life.⁷ Uremic polyneuropathy affects men more than women, and clinical signs include symmetric

¹Peripheral Neuropathy Unit, Centre for Clinical Translation, Department of Medicine, Imperial College London, Hammersmith Hospital, London, UK

²Nanomedicine Research Laboratory, Department of Medicine, Imperial College London, Hammersmith Hospital, London, UK

Corresponding Author:

P Anand, Peripheral Neuropathy Unit, Centre for Clinical Translation, Division of Brain Sciences, Imperial College London, Area A, Ground Floor, Hammersmith Hospital, Du Cane Rd, London W12 0NN, UK.
Email: p.anand@imperial.ac.uk



muscle weakness, areflexia and sensory loss of all modalities especially pin prick and vibration, with elevation of vibration threshold being an early sign.^{6,8} At the microscopic level, neuropathological lesions include destruction of myelin and axons with Wallerian degeneration.^{4,9,10}

The severity of neuropathy is strongly correlated with uraemia and associated with abnormalities of nerve conduction and excitability, including reduced sensory nerve action potentials; there is only partial and temporary improvement after haemodialysis.¹ Up to 90 uremic retention solutes or uremic toxins have been identified, which may interact negatively with biologic functions due to the progressive retention of solutes that would otherwise be excreted by healthy kidneys.¹¹ Of these, several predisposing factors to uremic neuropathy have been identified including elevated serum K^+ which affects motor axons more than sensory axons.¹² $TNF\alpha$ levels were also found to be significantly elevated in dialysis patients with neuropathy and left ventricular hypertrophy and considered to contribute to the development or maintenance of some neurologic and cardiac complications of uremic syndrome.¹³

Renal transplantation improves the clinical and electrophysiological signs even in severe uremic neuropathy and is recommended to be the only treatment for uremic neuropathy, indicating the role of a uremic toxin in the development of the neuropathy.^{5,10} As the mechanism of development of the neuropathy is not clear, and serum urea concentration is correlated with pre-dialysis nerve excitability parameters,¹ we examined the effect of treating cultured dorsal root ganglion (DRG) neurons with urea at concentrations described in cases of uremic neuropathy, i.e. higher than the normal range. Serum/plasma urea concentrations in patients with renal dysfunction can range from being mildly to severely increased, depending on the severity of the disease, with levels in patients undergoing dialysis for CKD exceeding 50 mMol/L.¹⁰ The normal range in human blood is between 2.5 and 6.7 mMol/L, though age-related increases in plasma urea levels of 14.3–17.8 mmol/L are also observed in healthy elderly individuals with no loss of renal function, due to decreased fractional urea excretion.¹⁴

Materials and methods

Neuron culture

Bilateral DRG from cervical, thoracic, lumbar and sacral levels of adult female Wistar rats (Charles River UK Ltd, Margate, Kent, UK) were microdissected, collected in Ham's F12 medium and enzyme digested in Ham's F12 nutrient medium containing 0.2% collagenase and 0.5% dispase for 3 h at 37°C, as previously

described.^{15,16} Enzyme digested tissue was triturated in BSF2 medium (containing 2% HIFCS, 0.1 mg/mL transferrin, 60 ng/mL progesterone, 0.16 µg/mL sodium selenite, 3 mg/mL bovine serum albumin (BSA), penicillin/streptomycin 100 µg/mL each, 16 µg/mL putrescine, 10 µg/mL insulin), soybean trypsin inhibitor and DNase to obtain a neuronal suspension. One rat was used for each experiment, and the neuron suspension was plated on several poly-l-lysine and laminin (20 µg/ml each) coated glass bottom MatTek dishes (MatTek Corp, USA) at 1000 neurons per dish for immunofluorescence studies, and 8000 neurons per dish for calcium imaging studies. BSF2 (2 ml) medium supplemented with 100 ng/ml of nerve growth factor (NGF) and 50 ng/ml glial cell line-derived neurotrophic factor (GDNF) and neurotrophin 3 (NT3) were added to all culture dishes and incubated at 37°C in a humidified environment of 5% CO_2 in air, until further study.

Urea was freshly prepared by dissolving in Ham's F12 culture medium at 100× final concentration, filter sterilized and added to the neuron cultures at 10 and 50 mmol/L, 24 h after plating, for immunofluorescence studies. Vehicle-treated controls had equivalent volume of medium added. Forty-eight hours after adding the urea, cultures were fixed in 2% paraformaldehyde (PFA) for 15 min.

Immunofluorescence

PFA fixed cultures from four rats were rinsed in phosphate-buffered saline (PBS) containing 0.01% sodium azide, permeabilized with methanol (−20°C, 3 min), rinsed with PBS and incubated in primary antibodies rabbit anti PGP9.5 (UltraClone, Cambridge, UK, 1:1000), mouse anti β III tubulin (Sigma, UK, 1:200), rabbit anti TRPV1 (1:300, GSK, Harlow, UK), rabbit anti TRPM8 (1:300, GSK, Harlow, UK), mouse monoclonal antibody to the neuronal marker Gap43 (1:200, Sigma, UK), for 1 h at room temperature, followed by 3 PBS rinses. Neurons were visualised by incubating in secondary antibodies, Alexa 546 (goat anti rabbit 1:400, Life Technologies, UK) and Alexa 488 (goat anti mouse 1:400, Life Technologies, UK), for 45 min at room temperature, and rinsed in PBS. The glass bottom was detached from the dish and mounted on a glass slide in glycerol containing the antifade agent DABCO [1,4-diazobicyclo-(2,2,2)-octane], and sealed with nail varnish. Tiff fluorescence images were acquired with a Photometrics HQ2 Coolsnap CCD camera, using standard wide-field fluorescence optics on a BX43 Olympus microscope with 20× and 60× oil objective lenses, and Cellsense software (Olympus, Japan), for morphological analysis, after confirming the absence of immunostaining in negative controls where the primary antibody had been omitted. The number of neurons

surviving were counted in each experimental group in three experiments, averaged and normalized to vehicle-treated neurons. Maximum neurite lengths were measured from Tiff images of individual PGP9.5 immunofluorescent neurons in each group, averaged and compared using Excel software. Numbers of TRPV1- and TRPM8-positive neurons were counted and expressed as a proportion of total Gap43-positive neurons.

Functional studies. Calcium imaging was used to determine the effect of acute urea application on the capsaicin sensitivity of DRG neurons in HEPES-buffered phenol-red free Hanks' Balanced Salt Solution, containing 0.1% BSA as previously described.^{16,17} Responses to paired capsaicin stimuli were measured in neurons loaded with 2 $\mu\text{Mol/L}$ Fura2 AM (Life Technologies, Paisley, UK) as a change in the baseline 340/380 λ_{ex} nm ratio before, during and after addition. Experiments were conducted at 37°C in a humidified environment on an inverted Nikon microscope (Diaphot 300; Nikon, UK Ltd, Kingston upon Thames, Surrey, UK) and cultures were alternately excited at 340 and 380 nm λ_{ex} wavelengths. Responses to paired capsaicin stimuli in individual neurons, with or without urea, were measured as the maximum change in the 340/380 λ_{ex} nm ratio from baseline. Images of 15 to 20 neurons in each experiment were captured every 2 s in each of three channels – brightfield, 340 and 380 nm λ_{ex} /510 λ_{em} – and recordings of intracellular changes in bound/unbound Ca^{2+} ratio were obtained before, during and after the addition of capsaicin. This provided baseline recordings as well as intracellular changes in Ca^{2+} levels in response to added capsaicin. Cells were uniformly loaded with the dye and no intracellular compartmentalization of the loaded dye was observed. Images were acquired with a Hamamatsu Orca CCD Camera and analysed with AQM Advance Kinetic imaging software. Individual cells under study were highlighted as regions of interest for calculating the mean ratios of bound to unbound calcium within the area of interest.

In each experiment, neurons were exposed to capsaicin for a maximum of two applications only, first to identify capsaicin sensitive neurons (using 200 nM capsaicin for 15 s), followed by washout and rest period of 45 min. The second stimulus of 1 μM capsaicin was used to test the effect of the added urea, mannitol or vehicle after the washout period. Only neurons responding to 200 nM capsaicin with a rapid and sustained increase in 340/380 ratio more than 20% from the baseline were selected for study. The second capsaicin stimulus of 1 $\mu\text{Mol/L}$ was applied after the baseline had returned to normal.

For calcium imaging experiments, urea was freshly dissolved in distilled water at 100 \times final concentration.

Capsaicin was dissolved in ethanol at 20 mmol/L concentration, aliquoted and stored at -20°C , and fresh aliquots were made up to 500 \times final concentration prior to use. Osmolality of solutions was confirmed using a vapour pressure osmometer. All chemicals were obtained from Sigma-Aldrich UK unless otherwise stated. Responses from individual neurons were averaged for individual rats in each group and Student's *t* test was used to compare between groups; data are presented as mean \pm S.E.M., * $P < 0.05$ was considered to be statistically significant (** $P < 0.01$ and *** $P < 0.001$). 'n' indicates the number of animals used for each group. SB705498 is a potent TRPV1 antagonist (gift from GSK, UK). LY294002 is a PI3 kinase inhibitor (Tocris, UK), PD98059 is a mitogen-activated protein kinase kinase (MEK) inhibitor (Tocris, UK) and AMTB is a TRPM8 inhibitor (Santacruz biotechnology, Germany).

Results

Morphological effects

Immunofluorescence for PGP9.5 in vehicle-treated neurons showed robust neurite outgrowth, with uniform staining in the soma and neurites (Figure 1(a) and (b)). Neurons treated with 10 mmol/L and 50 mmol/L urea for 48 h showed neurites with a beaded appearance indicating degeneration; the immunofluorescence was very bright in the cell soma but diminished in the neurites and terminals (Figure 1(c) and (f)).

Neurite tips of vehicle-treated neurons terminated in typical growth cones that were spread out with fine filopodia extensions (Figure 2(a) to (c)). The growth cones in urea-treated neurons had retracted and were present as swollen end bulbs, with loss of filopodia (Figure 2(d) to (f)). These effects were evident in the 10 mmol/L-treated neurons and were more pronounced in the 50 mmol/L urea-treated cultures, which also showed vesiculated neurites.

Double immunofluorescence in vehicle-treated neurons showed uniformly and diffusely distributed PGP9.5 co-localized with β III tubulin (Figures 3 and 4).

Neurons treated with urea showed pale, diminished and patchy PGP9.5 expression, with fibrillar aggregates of β III tubulin especially in the growth cones (Figures 3 and 4). Neurons in advanced stages of degeneration had vesiculated growth cones.

TRPM8-positive neurons (Figure 5(a) to (c)) were smaller than TRPV1-positive neurons (Figure 5(d) to (f)). Neurite lengths were reduced in neurons treated with urea for 48 h, compared with the average maximum neurite length from vehicle-treated control neurons being $476 \pm 55 \mu\text{m}$ ($n = 4$, 99 neurons), reduced to $286 \pm 12 \mu\text{m}$ ($n = 4$, 166 neurons ** $P < 0.01$) after 10 mmol/L

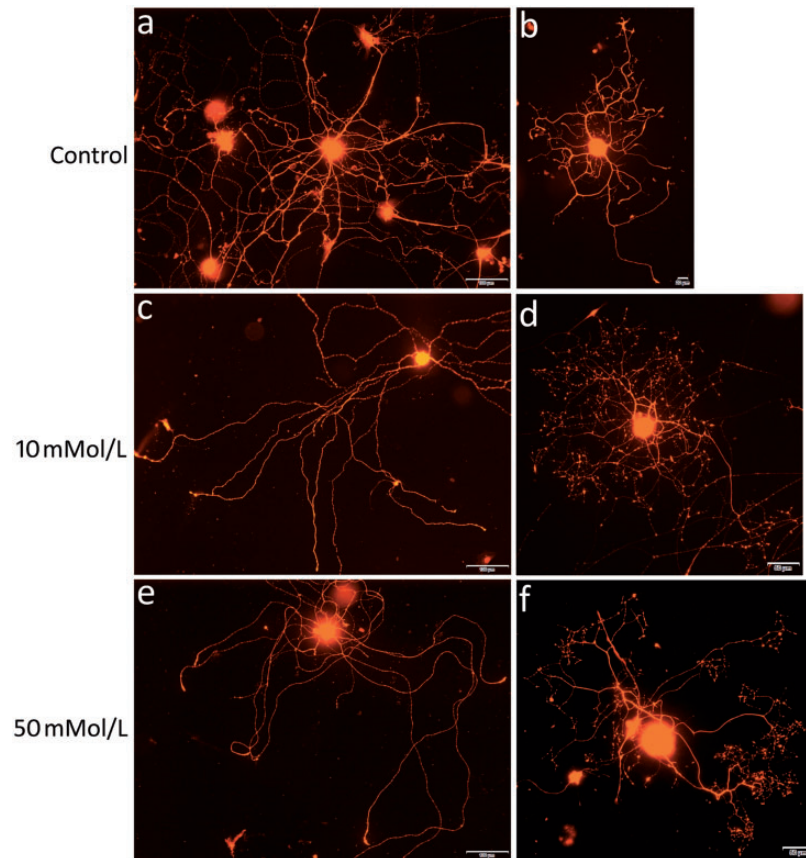


Figure 1. Examples of neurite degeneration in urea-treated neurons. PGP9.5 immunofluorescence showing vehicle-treated neurons with robust, uniformly stained neurite outgrowth (a, b), while neurons treated with 10 mmol/L (c, d) or 50 mmol/L (e, f) urea show depleted staining in degenerating neurites but increased staining intensity in the soma. Bar in (a), (c) and (e) = 100 μ m; (b) = 20 μ m; (d) and (f) = 50 μ m.

urea treatment, and to $268 \pm 16 \mu\text{m}$ ($n = 4$, 152 neurons, $**P < 0.01$) after 50 mmol/L urea treatment (Figure 5(g)).

Significantly reduced numbers of neurons were observed to survive after treatment with urea, compared with vehicle treatment. The proportion of surviving neurons after 48 h incubation with 10 mmol/L urea was reduced to $70.08 \pm 13.3\%$ ($n = 3$, total 930 neurons, $*P < 0.05$, Student's paired t test) and to $61.49 \pm 7.4\%$ after 50 mmol/L treatment ($n = 3$, total 816 neurons, $**P < 0.01$ Student's paired t test), compared with vehicle-treated neurons ($100 \pm 1.6\%$, $n = 3$, total 1327 neurons) (Figure 5(h)).

Double immunofluorescence for TRPV1 and Gap43 in neurons treated with urea or vehicle for 24 h showed that $67.7 \pm 3.2\%$ neurons were double labelled for Gap43 and TRPV1 in vehicle-treated controls, while $66.2 \pm 2.3\%$ were TRPV1 positive after 10 mmol/L, and reduced to $53.8 \pm 12.4\%$ after 50 mmol/L urea for 24 h. Similarly, double labelling for TRPM8 and Gap43 showed $11.6 \pm 4.8\%$ neurons positive for TRPM8 in control neurons, while $19.6 \pm 2.9\%$ were TRPM8

positive after 10 mmol/L urea and $23 \pm 5.5\%$ were TRPM8 positive after 50 mmol/L urea treatment (Figure 5(i)).

Functional effects

Calcium imaging showed that vehicle-treated neurons demonstrated a robust response to 200 nMol/L capsaicin (Figure 6(a)), with a smaller second response to 1 μ Mol/L capsaicin after the 45-min washout and rest period (Figure 6(b)). Neurons treated with 10 or 50 mmol/L urea for 10 min, between the two capsaicin stimuli, showed an increased second response, compared with the first, indicating sensitization (Figure 6(c) to (f)). In addition, neurons treated with urea for 48 h showed sluggish, smaller responses to 200 nMol/L capsaicin than vehicle-treated neurons, and previously unresponsive or weakly responsive neurons responded robustly to 1 μ Mol/L capsaicin after acute urea application (Figure 6(g) and (h), data not quantified). Neurons treated with 10 or 50 mmol/L mannitol did not demonstrate sensitization of capsaicin responses.

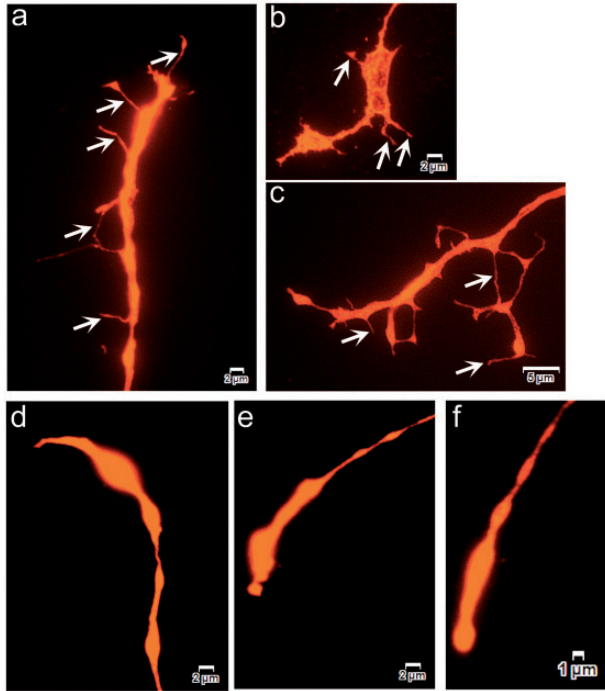


Figure 2. Growth cone morphology. Images of PGP9.5 immunofluorescence in adult rat DRG neurons show growth cones in vehicle-treated neurons with multiple fine filopodia (arrows in (a), (b) and (c)), while neurons treated with urea for 48 h have swollen retracted growth cones with loss of filopodia ((d), (e) and (f)).

The percentage change in the second response compared with the first response for each neuron was averaged for each experiment for the different groups and normalized to vehicle-treated neurons (Figure 7(a), bar 1, $100 \pm 4.2\%$, $n = 7$, 33 neurons).

Capsaicin responses in the presence of 10 mmol/L mannitol were similar to vehicle control (Figure 7(a), bar 2, $100.8 \pm 7\%$, $n = 7$, 31 neurons, n.s.) and reduced with 50 mmol/L mannitol (Figure 7(a), bar 3, $76.6 \pm 6.7\%$, $n = 3$, 29 neurons). Sensitization of capsaicin responses was maintained in the presence of 10 mmol/L urea applied after incubation with 3 $\mu\text{mol/L}$ thapsigargin (smooth endoplasmic reticulum calcium pump inhibitor) (Figure 7(a), bar 4, $135.8 \pm 8.6\%$, $n = 4$, 11 neurons, $**P < 0.01$). Moreover, 10 mmol/L urea applied in calcium- and magnesium-free extracellular medium reduced capsaicin responses in DRG neurons (Figure 7(a), bar 5, $68.4 \pm 15.6\%$, $n = 3$, 21 neurons, n.s. compared with vehicle-treated controls and $**P < 0.01$ compared with 10 mmol/L urea in medium containing calcium and magnesium).

Quantitation of data in the graph (Figure 7(b)) shows that capsaicin sensitivity was increased after acute treatment with 10 mmol/L urea, to $115.29 \pm 3.4\%$ (bar 2, $n = 6$, 45 neurons, $**P < 0.01$), that was reduced to

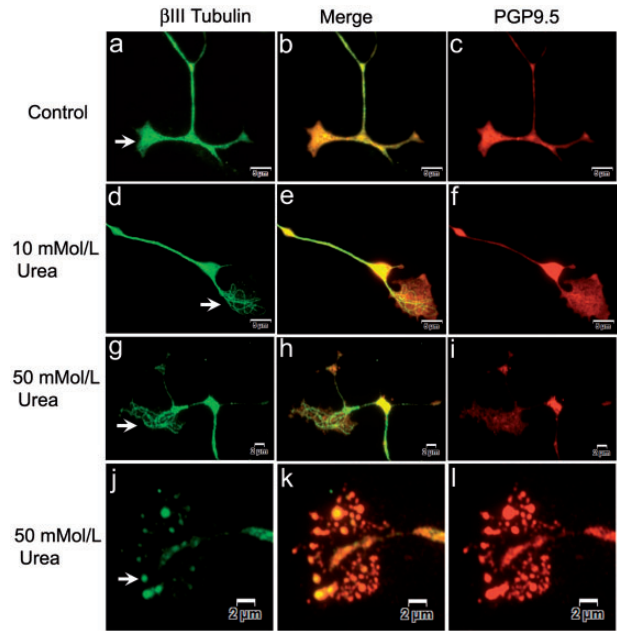


Figure 3. β III tubulin and PGP9.5 expression in growth cones. Widefield immunofluorescence showing growth cones of vehicle-treated neurons with uniformly distributed β III tubulin (arrow in a, green), appearing yellow in the merged image (b) and overlapping the PGP9.5 expression (c, red). After 48 h 10 mmol/L urea treatment, neurons show growth cones containing distinct thickened β III tubulin-positive fibres (d, green), with the merged image in (e), and pale depleted PGP9.5 expression (f, red). Similarly, 50 mmol/L urea-treated neurons show thickened individual β III tubulin-positive fibres in the growth cone (g, green), merged image (i, yellow) and pale depleted PGP9.5 (h, red). Vesiculated remnants of the degenerating growth cone contain β III tubulin (j, green), merged image (k, yellow) and PGP9.5 (l, red). Bar (a) to (f) = 5 μm , (g) to (l) = 2 μm .

$66.1 \pm 3.5\%$ in the presence of 30 $\mu\text{mol/L}$ TRPM8 inhibitor AMTB (bar 3, $n = 3$, 24 neurons, $***P < 0.001$), reduced to $55.7 \pm 7.5\%$ in the presence of 1 $\mu\text{mol/L}$ MEK inhibitor PD98059 (bar 4, $n = 3$, 17 neurons, $***P < 0.001$), and reduced to $51 \pm 9.9\%$ in the presence of 1 $\mu\text{mol/L}$ PI3 kinase inhibitor LY294002 (bar 5, $n = 3$, 26 neurons, $***P < 0.001$).

Dose-related sensitization of capsaicin responses was observed after acute application of 50 mmol/L urea to $125.3 \pm 4.2\%$ (Figure 7(b), bar 6, $n = 4$, 30 neurons, $**P < 0.01$) that was reduced to $56.2 \pm 9.5\%$ in the presence of the TRPV1 inhibitor SB705498 (Figure 7(b), bar 7, $n = 4$, 21 neurons, $***P < 0.001$).

Discussion

As elevated serum urea is the prominent underlying feature of progressive decline in kidney function, leading to CKD and consequent uremic neuropathy, we sought to determine the effects of urea treatment on cultured sensory neurons from adult rats. The urea concentrations

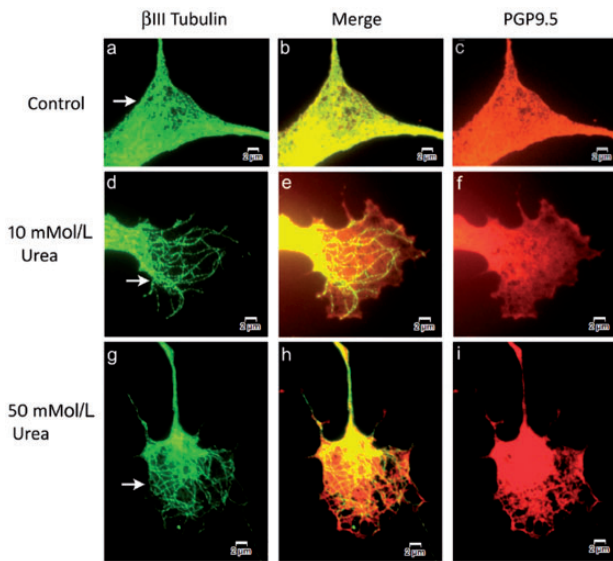


Figure 4. Similar to Figure 3. Higher magnification images of β III tubulin and PGP9.5 expression in growth cones. Wide-field immunofluorescence showing growth cones of vehicle-treated neurons with uniformly distributed β III tubulin (a, green), appearing yellow in the merged image (b, yellow), co-expressed with PGP9.5 (c, red). After 48 h 10 mMol/L urea treatment, neurons show growth cones containing distinct thickened β III tubulin-positive fibres (arrows in d, green), the merged image (e) and pale depleted PGP9.5 expression (f, red). Similarly, 50 mMol/L urea-treated neurons show thickened individual β III tubulin-positive fibres in the growth cone (arrows in g, green), merged image (h, yellow) and patchy PGP9.5 (i, red). Bar = 2 μ m.

used in our study are based on clinical reports, where the normal range in human blood is 2.5 to 6.7 mMol/L. Higher serum concentrations have been previously reported with $C_{\max} = 4.6$ g/L,¹¹ which equates to 152.25 mMol/L, and blood urea nitrogen of 157 mg/dl/L,¹⁰ equal to 58.87 mMol/L, which are higher than the concentrations used in our study. We tested the effect of urea on the morphology and function of sensory neurons, and our observations indicate that sensory neurons exposed to urea at levels observed in conditions of uremic neuropathy, above the normal blood urea levels, demonstrate hypersensitivity followed by neurite degeneration.

Previous studies have described the pathology of uremic neuropathy, with axonal dying-back and demyelination as predominant and consistent features in patients with CKD. These morphological changes are concomitant with functional changes in nerve conduction, reduced action potentials and loss of tendon reflexes, features that are common in peripheral neuropathy. Our morphological findings, of neurite degeneration characterized by swollen degenerating growth cones with loss of filopodia in urea-treated neurons, provide a

mechanistic basis for this condition. The neurotoxic action of high levels of urea compromises neuronal structure and function. Structural integrity was compromised by the loss of filopodia, which are fine, dynamic, actin and myosin-rich finger-like structures in the growth cones at the tips of growing neurites. Filopodia have a sensory function and respond to guidance cues in their environment, essential for neurite growth, synapse formation and maintenance, under the regulation of a number of different proteins.¹⁸ The pattern of loss of filopodia, combined with neurite and growth cone degeneration, may be attributed to generalized toxic effects, with the potential to affect other types of neurons, including motoneurons. This may underlie features such as the acute partial denervation and loss of motor units in weak muscles observed in uremic neuropathy.⁸

Intracellular effects of urea treatment were apparent with double immunofluorescence using specific antibodies for the neuronal marker PGP9.5, a member of the ubiquitin C-terminal hydroxylase family, which showed diffuse distribution and co-expression with β III tubulin in control neurons. The depletion of PGP9.5 in the neurites of urea-treated neurons and concentration in the cell soma suggests impaired axonal transport mechanism or depletion from the neurite tips towards the cell body. While the β III tubulin was uniformly distributed in vehicle-treated neurons, it appeared as bundles or aggregated distinct fibrillar structures, progressing to degenerating vesicles replacing the growth cones of urea-treated neurons. β III tubulin is a major constituent of microtubules, and mutations in β III tubulin are associated with peripheral neuropathy, due to loss of axons and disruption of axon transport of Rab3A, a synaptic vesicle associated small GTPase.¹⁹ The importance of microtubules in maintaining growth cone structure was demonstrated in cultured DRG neurons treated with the microtubule disrupting agent nocodazole, which resulted in the loss of growth cones and formation of retraction bulbs.²⁰ Growth cones of normal DRG neurons cultured with low-dose NGF contain β III tubulin-positive microtubules associated with kinesin.²¹ However, we observed microtubule bundles in urea-treated neurons, whereas control neurons showed diffuse and co-localized distribution of β III tubulin and PGP9.5. The presence of GDNF in addition to NGF is reported to significantly increase the thickness and size of neurite terminals²² and our observation of microtubule bundles in urea-treated neurons may be due to thinning of the plasma membrane, or to inactivation of the neurotrophic factors by the proteolytic action of urea, as described below. In our previous study, the neurodegenerative effects of the *Mycobacterium Ulcerans* toxin mycolactone in cultured DRG neurons included loss of β III tubulin accompanied by TRPV1 desensitization,²³ while this study shows the opposite effect, of β III tubulin aggregation accompanied

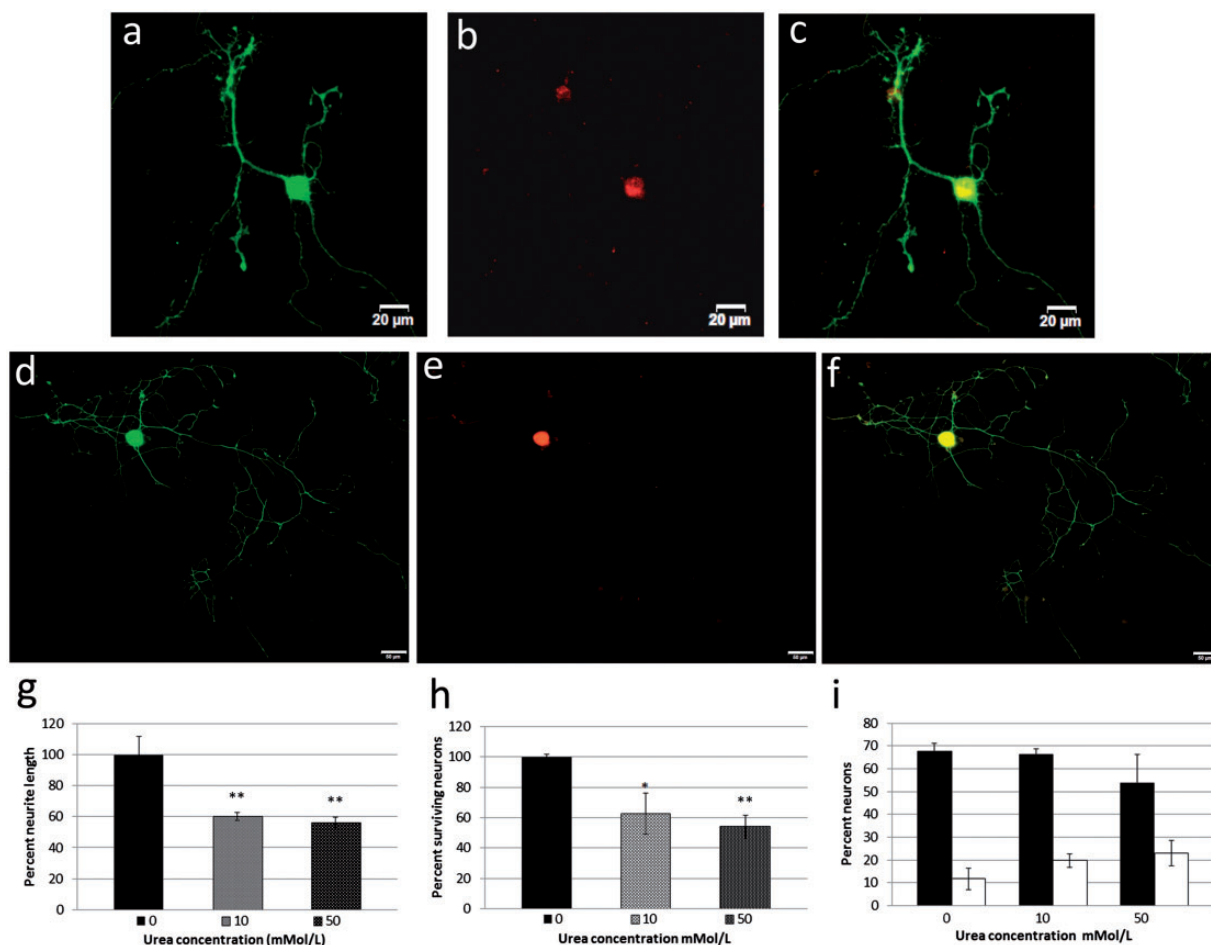


Figure 5. Effect of urea treatment on neurite length, neuron number and expression of TRPV1 and TRPM8 in cultured DRG neurons. Sample images of neurons showing double immunofluorescence for Gap43 in the soma and neurites (green, a) and TRPM8 in the soma (red, b), and merged image in (c) Bar = 20 μ m. Similar Gap43 (green, d) and TRPV1 (red, e), with merged image in (f) Bar = 50 μ m. Graph showing reduced neurite lengths of neurons treated with 10 or 50 mmol/L urea normalized to vehicle-treated control (0) (g). Graph showing reduced number of surviving neurons after 10 and 50 mmol/L urea normalized to control (h). Graph of percent neurons expressing TRPV1 (black bars), and TRPM8 (clear bars), double labelled with Gap43 (i).

by neuronal sensitization, suggesting a common pathway influencing TRPV1 receptor activation and tubulin stability that requires elucidation.

Our results from immunofluorescence studies on neurite length and number show that significant neurite and neuron loss can occur at the lower dose of 10 mmol/L urea, and the effects were slightly increased at the higher dose of 50 mmol/L, consistent with the pathology of uremic neuropathy.

Previous studies have provided a range of values for the proportion of DRG neurons expressing TRPV1: $46.9 \pm 1.6\%$,²⁴ $46.8 \pm 2.2\%$,²⁵ $42 \pm 6\%$,²⁶ $58 \pm 2\%$,²⁷ and $42 \pm 7\%$ ²⁸ and TRPM8: 4.7% ,²⁹ $5\%–10\%$,^{30,31} 12.9% ,³² and 22.8% .²⁴ Our TRPV1-positive neuron numbers were higher, as observed in animal models of inflammation^{33,34} and in clinical conditions of chronic pain,^{35–37} also reflecting the effect of added neurotrophic

factors in culture.¹⁷ Our study also showed a dose-related loss of TRPV1-positive neurons in the urea-treated group (n.s.), indicating susceptibility of TRPV1 expressing neurons to urea, and a small relative increase (n.s.) in TRPM8-positive neurons, possibly reflecting the loss of TRPV1 neurons.

The functional effect of neuronal sensitization was apparent after acute incubation with urea and preceded the morphological effects of neurite degeneration observed after 48 h incubation with urea. Sensitization of capsaicin responses is the opposite of the expected reduction in the second response due to tachyphylaxis, which normally provides a protective mechanism, allowing neurons a period of recovery after stimulation and calcium influx. Thus, the sensitization shown by increased intracellular calcium on capsaicin stimulation indicates increased neuronal excitability due to increased

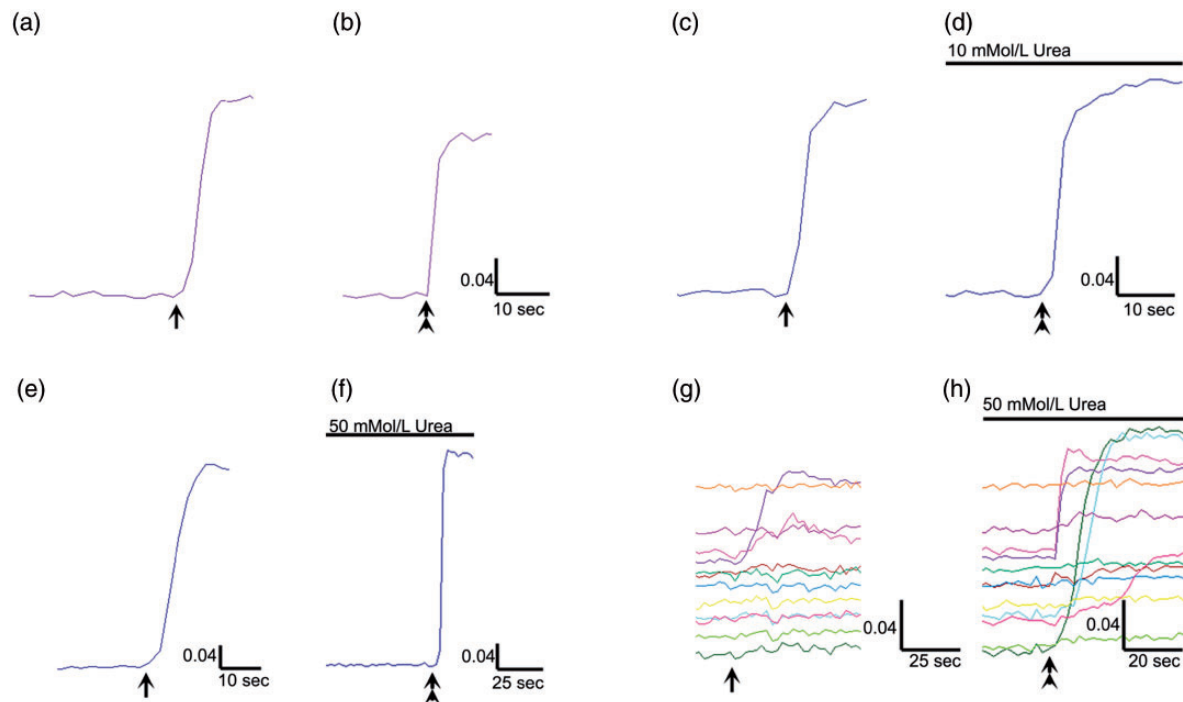


Figure 6. Effects of urea on capsaicin sensitivity. Sample trace of calcium influx in response to 200 nMol/L capsaicin (arrow, a). Following washout and rest period of 45 min, a second application of capsaicin (1 μMol/L, double arrowhead, b) results in a smaller response, in a vehicle-treated neuron. The first response to 200 nM capsaicin in a different neuron (arrow, c), followed by 10 mmol/L urea applied for 10 min, at the end of the washout and 45-min rest period, results in enhanced calcium influx in response to 1 μMol/L capsaicin (double arrowhead, d). Similar traces showing the first response to 200 nM capsaicin in a different neuron (arrow, e), and the enhanced response to 1 μMol/L capsaicin (double arrowhead, f), in the presence of 50 mmol/L urea. Responses to 200 nMol capsaicin in neurons after 48 h incubation with 50 mmol/L urea (g), and previously unresponsive neurons showing robust responses after acute application of 50 mmol/L urea (h). Scale bars indicate time in seconds on the X axis, and change in mean 340/380 intensity ratio on the Y axis.

calcium influx or release from intracellular stores, or both; our findings of the absence of sensitization in calcium-free medium, and its persistence in the presence of thapsigargin, indicate increased calcium influx in the presence of urea, rather than calcium release from intracellular stores. We used capsaicin to study activation of TRPV1, the neuronal receptor involved in sensing noxious stimuli leading to the perception of pain,³⁸ to mimic endogenous agonists of this receptor that are likely to have similar effects, especially in inflammatory conditions. The resulting increase in intracellular calcium levels in urea-treated neurons and loss of calcium homeostasis would be expected to lead to altered sensitivity and structural degeneration characteristic of uremic neuropathy. In a previous study, exposure of human neuroblastoma cells to urea at clinically relevant concentrations (40–200 mg/dl) resulted in the expression of heat shock proteins and protein carbamylation but not after exposure to equivalent concentrations of mannitol, creatinine, or glycerol, suggesting neurotoxicity of urea.³⁹ Contrary to the findings of Liu et al.,⁴⁰ we did not observe sensitization of neurons to capsaicin in

hypertonic medium (containing 10 mmol/L or 50 mmol/L mannitol), though, similar to their findings, we observed absence of calcium influx in response to hypertonic stimuli and elimination of sensitization by the PI3K inhibitor. In addition, we have demonstrated the efficacy of the TRPM8 inhibitor and the MEK kinase inhibitor in eliminating urea-mediated neuronal sensitization. It is likely that the differences in our results are due to different temperatures at which experiments were conducted and the neuronal population under study, as Liu et al.⁴⁰ performed their study on trigeminal neurons at 22°C to 24°C, while our experiments were conducted on DRG neurons at 37°C.

Urea is one of many components including TNFα that are increased in the plasma of individuals with CKD,¹¹ which may have a synergistic effect. Sensitization in the presence of urea may be due to a change in osmolality, but is unlikely, as solutes such as urea equilibrate across the cell membrane and do not cause cellular dehydration.⁴¹ Quallo et al.²⁹ reported that hyperosmolality evoked calcium influx in TRPM8 expressing DRG, Trigeminal ganglia (TG) and TRPM8

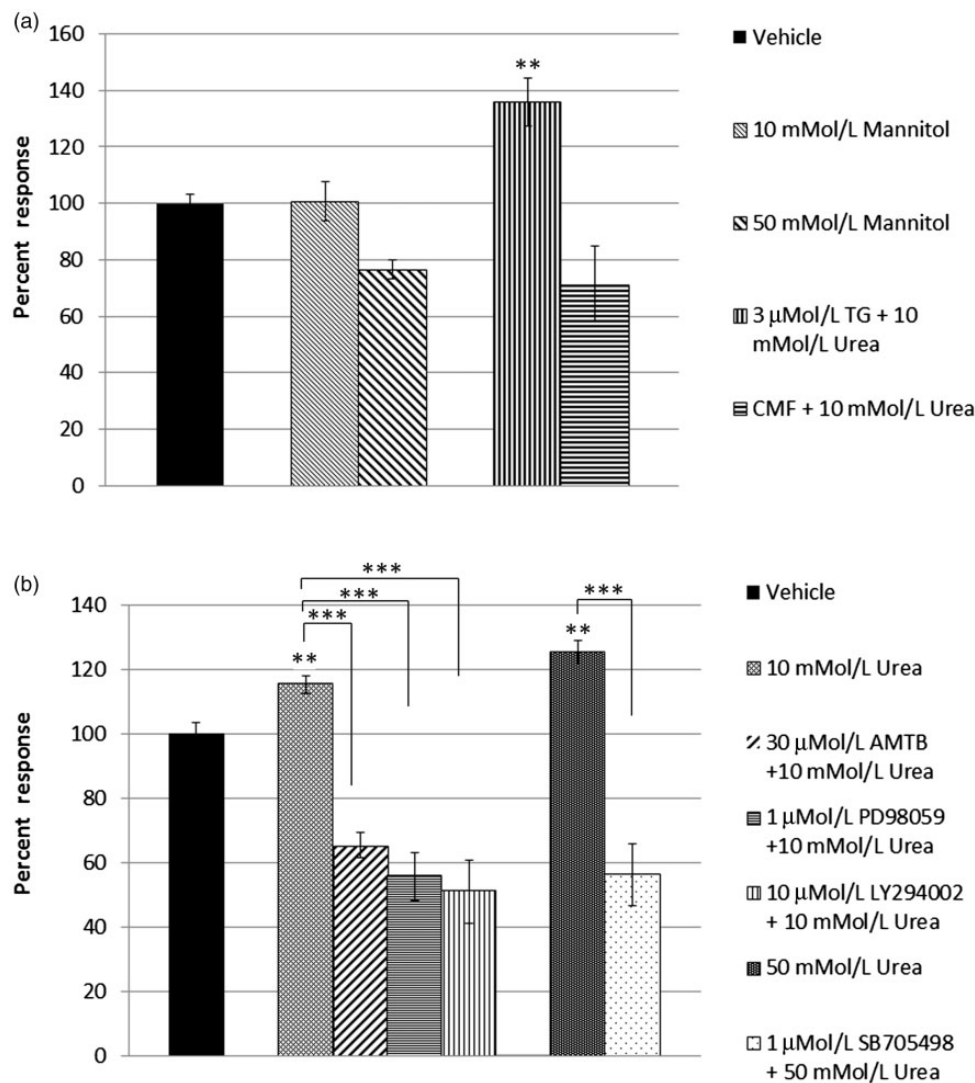


Figure 7. (a) Graph showing capsaicin responses in vehicle-treated neurons (1st bar, black), and equivalent responses after 10 mmol/L mannitol (bar 2, n.s.), and after 50 mmol/L mannitol incubation (bar 3). Urea-mediated sensitization was preserved after thapsigargin (TG) treatment (bar 4, $^{**}P < 0.01$), but not in calcium- and magnesium-free extracellular medium (CMF) (bar 5). (b) Acute effect of urea on capsaicin sensitivity in cultured DRG neurons. Capsaicin responses in vehicle-treated neurons (first bar, black); capsaicin sensitivity was significantly increased after acute application of 10 mmol/L urea (bar 2), which was inhibited in the presence of inhibitors of TRPM8 N-(3-Aminopropyl)-2-[(3-methylphenyl)methoxy]-N-(2-thienylmethyl)benzamide (AMTB hydrochloride) (bar 3), MAP kinase PD98059 (bar 4), and PI3 kinase LY294002 (bar 5). Dose-related sensitization in the presence of 50 mmol/L urea (bar 6) was diminished by the TRPV1 inhibitor SB705498 (bar 7, $^{***}P < 0.001$).

transfected cells, which were temperature sensitive and observed at lower temperatures than used in our study, with a low threshold of activation (27°C) and having decreasing response amplitude with temperature increasing to 37°C . Our experiments were conducted at 37°C , and we did not observe calcium influx in response to urea or mannitol application at the concentrations and temperature conditions used. Thus, TRPM8 may be activated by hyperosmolality and play a predominant role where the physiological temperature is appropriate for TRPM8 activation as in corneal afferents, shown by

Quallo et al.²⁹ The inhibitory effect of the TRPM8 inhibitor AMTB in our study indicates a common pathway in TRPV1 and TRPM8 activation, reflecting co-expression of these two receptors in DRG neurons. Our study examined the effect of urea at the concentrations observed in conditions of uremic neuropathy and its potential effects on TRPV1 to understand the mechanistic basis of the associated pain and paraesthesia. Whether urea has similar sensitizing effects on other ion channels involved in nociception remains to be determined.

One of the mechanisms influencing neuronal sensitization involves TRPV1 phosphorylation by elevated cAMP,^{42,43} with the activation of protein kinase A and other kinases in nociceptive afferents, resulting in hyperalgesia.^{44–46} Urea appears to have a synergistic effect in this pathway, as the sensitizing effect mediated by urea was eliminated by the MEK inhibitor PD 98059 and the PI3 kinase inhibitor LY 294002. Partial inhibition by the high concentration of the TRPM8 inhibitor AMTB likely demonstrates its effect on TRPV1 and TRPM8 co-expressing neurons, as co-expression is reported to occur in the presence of NGF,⁴⁷ as in our study. Although TRPM8 and TRPV1 expression was initially reported in non-overlapping subsets of DRG neurons,²⁴ others have described their co-expression in a subpopulation of neurons.^{32,48} The MEK inhibitor PD98059 and the PI3 kinase inhibitor LY294002 inhibited urea-mediated sensitization to a greater extent at low doses, as did the TRPV1 inhibitor SB705498. Thus, reversal of elevated cAMP by MEK/PI3 kinase inhibitors, TRPV1 antagonists, or maintenance of plasma osmolality below 10 mmol/L may provide effective strategies in preventing urea-mediated neuronal sensitization and degeneration.

The neurodegenerative effects of urea may be explained by its chaotropic property, which renders it useful as a protein denaturing agent for studies of protein analysis, by protein unfolding, due to unravelling the tertiary structure by destabilizing internal, non-covalent bonds. Protein denaturation by urea can also proceed via direct interaction of urea by forming hydrogen bonds with polarized areas of charge, such as peptide groups, weakening intermolecular bonds, and the overall secondary and tertiary structure, although this has been described at molar concentrations.⁴⁹ Urea diffuses easily due to its small molecular size aiding its distribution in total body water and also acts as a humectant by absorbing water. These properties form the basis of commercially available topical formulations as keratolytic agents. While our findings describe the direct effects of elevated urea on DRG neurons, significant autonomic and central nervous system effects are also associated with uremia. Uremic encephalopathy occurs in patients with renal failure due to the accumulation of urea in the brain.^{50,51} Atrophy of the striatum is characteristic of Huntington's disease (HD) pathology, where localized accumulation of urea is considered to be the primary biochemical basis for initiating neuropathogenesis.⁵² Widespread elevation of urea has been described in Alzheimer's disease brain tissue⁵³ and in brain tissue of patients with HD, indicating a role for dysregulated urea metabolism in neurodegeneration.⁵⁴

Our study provides a disease-related model of uremic neuropathy, offering insight into the pathogenesis of the condition, and the opportunity to test novel

agents to alleviate hypersensitivity and promote nerve regeneration.

Declaration of Conflicting Interests

The author(s) declared no potential conflicts of interest with respect to the research, authorship, and/or publication of this article.

Funding

The author(s) disclosed receipt of the following financial support for the research, authorship, and/or publication of this article: The authors thank the Biomedical Research Centre, Imperial College London, for facilities.

ORCID iD

U Anand  <https://orcid.org/0000-0002-3704-4600>

References

1. Krishnan AV, Phoon RKS, Pussell BA, Charlesworth JA, Kiernan MC. Sensory nerve excitability and neuropathy in end stage kidney disease. *J Neurol Neurosurg Psych* 2006; 77: 548–551.
2. Brouns R, De Deyn PP. Neurological complications in renal failure: a review. *Clin Neurol Neurosurg* 2004; 107: 1–16.
3. Asbury AK, Victor M, Adams RD. Uremic polyneuropathy. *Arch Neurol* 1963; 8: 413–428.
4. Asbury AK. Uremic polyneuropathy. In: Dyck PJ and Thomas PK (eds) *Peripheral neuropathy*. 3rd ed. Philadelphia, PA: WB Saunders 1993, pp. 1251–1257.
5. Bolton CF. Peripheral neuropathies associated with chronic renal failure. *Can J Neurol Sci* 1980; 789–796.
6. Ramirez BV, Bustamante-Gomez PA. Uraemic neuropathy: a review. *Int J Genet Mol Biol* 2012; 3: 155–160.
7. Yu XZ, Lu S, Gou W, Wang W, Zou SH, Han YX, Wang WW, Zhang JY. Assessment of the characteristics and quality of life of patients with uremic peripheral neuropathy. *Clin Nephrol* 2017; 87: 134–139.
8. Galassi G, Ferrari S, Rizzuto N. Neuromuscular complications of kidney diseases. *Nephrol Dial Transplant* 1998; 13: 41–47.
9. Dyck PJ, Johnson WJ, Lambert EH, O'Brien PC. Segmental demyelination secondary to axonal degeneration in uremic neuropathy. *Mayo Clin Proc* 1971; 46: 400–431.
10. Ho DT, Rodig NM, Kim HB, Lidov HGW, Shapiro FD, Raju GP, Kang PB. Rapid reversal of uremic neuropathy following renal transplantation in an adolescent. *Pediatr Transplant* 2012; 16: E296–E300.
11. Vanholder R, De Smet R, Glorieux G, Argilés A, Baurmeister U, Brunet P, Clark W, Cohen G, De Deyn PP, Deppisch R, Descamps-Latscha B, Henle T, Jörres A, Lemke HD, Massy ZA, Passlick-Deetjen J, Rodriguez M, Stegmayr B, Stenvinkel P, Tetta C, Wanner C, Zidek W, European Uremic Toxin Work Group (EUTox). Review on uremic toxins: classification,

- concentration, and interindividual variability. *Kidney Int* 2003; 63: 1934–1943.
12. Bostock H, Walters RJ, Andersen KV, Murray NM, Taube D, Kiernan MC. Has potassium been prematurely discarded as a contributing factor to the development of uremic neuropathy? *Nephrol Dial Transplant* 2004; 19: 1054–1057.
 13. Espinoza M, Aguilera A, Auxiliadora Bajo M, Codoceo R, Caravaca E, Cirugeda A, del Peso G, Hevia C, Selgas R. Tumor necrosis factor alpha as a uremic toxin: correlation with neuropathy, left ventricular hypertrophy, anemia, and hypertriglyceridemia in peritoneal dialysis patients. *Adv Perit Dial* 1999; 15: 82–86.
 14. Musch W, Verfaillie L, Decaux G. Age-related increase in plasma urea level and decrease in fractional urea excretion: clinical application in the syndrome of inappropriate secretion of antidiuretic hormone. *Clin J Am Soc Nephrol* 2006; 1: 909–914.
 15. Anand U, Otto WR, Sanchez-Herrera D, Facer P, Yiangou Y, Korchev Y, Birch R, Benham C, Bountra C, Chessell IP, Anand P. Cannabinoid receptor CB2 localisation and agonist-mediated inhibition of capsaicin responses in human sensory neurons. *Pain* 2008; 138: 667–680.
 16. Anand U, Otto WR, Anand P. Sensitization of capsaicin and icilin responses in oxaliplatin treated adult rat DRG neurons. *Mol Pain* 2010; 6: 1744-8069-6-82
 17. Anand U, Otto WR, Casula MA, Day NC, Davis JB, Bountra C, Birch R, Anand P. The effect of neurotrophic factors on morphology, TRPV1 expression and capsaicin responses of cultured human DRG sensory neurons. *Neurosci Lett* 2006; 399: 51–56.
 18. Mattila PK, Lappalainen P. Filopodia: molecular architecture and cellular functions. *Nat Rev Mol Cell Biol* 2008; 9: 446–454.
 19. Niwa S, Takahashi H, Hirokawa N. β -tubulin mutations that cause severe neuropathies disrupt axonal transport. *Embo J* 2013; 32: 1352–1364.
 20. Erturk A, Hellal F, Enes J, Bradke F. Disorganized microtubules underlie the formation of retraction bulbs and the failure of axonal regeneration. *J Neurosci* 2007; 27: 9169–9180.
 21. Gumy LF, Chew DJ, Tortosa E, Katrukha EA, Kapitein LC, Tolkovsky AM, Hoogenraad CC, Fawcett JW. The kinesin-2 family member KIF3C regulates microtubule dynamics and is required for axon growth and regeneration. *J Neurosci* 2013; 33: 11329–11345.
 22. Klusch A, Gorzelanny C, Reeh PW, Schmelz M, Petersen M, Sauer SK. Local NGF and GDNF levels modulate morphology and function of porcine DRG neurites, In Vitro. *PLoS One* 2018; 13: e0203215.
 23. Anand U, Sinisi M, Fox M, MacQuillan A, Quick T, Korchev Y, Bountra C, McCarthy T, Anand P. Mycolactone-mediated neurite degeneration and functional effects in cultured human and rat DRG neurons: mechanisms underlying hypoalgesia in Buruli ulcer. *Mol Pain* 2016; 12: 1–11.
 24. Kobayashi K, Fukuoka T, Obata K, Yamanaka H, Dai I, Tokunaga A, Noguchi K. Distinct expression of TRPM8, TRPA1, and TRPV1 mRNAs in rat primary afferent neurons with A/C-fibers and colocalization with Trk receptors. *J Comp Neurol* 2005; 493: 596–606.
 25. Michael GJ, Priestley JV. Differential expression of the mRNA for the vanilloid receptor subtype 1 in cells of the adult rat dorsal root and nodose ganglia and its downregulation by axotomy. *J Neurosci* 1999; 19: 1844–1854.
 26. Ahluwalia J, Urban L, Capogna M, Bevan S, Nagy I. Cannabinoid 1 receptors are expressed in nociceptive primary sensory neurons. *Neuroscience* 2000; 100: 685–688.
 27. Guo A, Simone DA, Stone LS, Fairbanks CA, Wang J, Elde R. Developmental shift of vanilloid receptor 1 (VR1) terminals into deeper regions of the superficial dorsal horn: correlation with a shift from TrkA to Ret expression by dorsal root ganglion neurons. *Eur J Neurosci* 2001; 14: 293–304.
 28. Carlton SM, Hargett GL. Stereological analysis of Ca²⁺/calmodulin-dependent protein kinase II alpha -containing dorsal root ganglion neurons in the rat: colocalization with isolectin Griffonia simplicifolia, calcitonin gene-related peptide, or vanilloid receptor 1. *J Comp Neurol* 2002; 448: 102–110.
 29. Quallo T, Vastani N, Horridge E, Gentry C, Parra A, Moss S, Viana F, Belmonte C, Andersson DA, Bevan S. TRPM8 is a neuronal osmosensor that regulates eye blinking in mice. *Nat Commun* 2015; 6: 7150.
 30. Peier AM, Moqrich A, Hergarden AC, Reeve AJ, Andersson DA, Story GM, Earley TJ, Dragoni I, McIntyre P, Bevan S, Patapoutian A. A TRP channel that senses cold stimuli and menthol. *Cell* 2002; 108: 705–715.
 31. Dhaka A, Murray AN, Mathur J, Earley TJ, Petrus MJ, Patapoutian A. TRPM8 is required for cold sensation in mice. *Neuron* 2007; 54: 371–378.
 32. Takashima Y, Daniels RL, Knowlton W, Teng J, Liman ER, McKemy DD. Diversity in the neural circuitry of cold sensing revealed by genetic axonal labeling of transient receptor potential melastatin 8 neurons. *J Neurosci* 2007; 27: 14147–14157.
 33. Carlton SM, Coggeshall RE. Peripheral capsaicin receptors increase in the inflamed rat hindpaw: a possible mechanism for peripheral sensitization. *Neurosci Lett* 2001; 310: 53–56.
 34. Amaya F, Oh-Hashi K, Naruse Y, Iijima N, Ueda M, Shimosato G, Tominaga M, Tanaka Y, Tanaka M. Local inflammation increases vanilloid receptor 1 expression within distinct subgroups of DRG neurons. *Brain Res* 2003; 963: 190–196.
 35. Chan CLH, Facer P, Davis JB, Smith GD, Egerton J, Bountra C, Williams NS, Anand P. Sensory fibres expressing capsaicin receptor TRPV1 in patients with rectal hypersensitivity and faecal urgency. *Lancet* 2003; 361: 385–391.
 36. Tympanidis P, Casula MA, Yiangou Y, Terenghi G, Dowd P, Anand P. Increased vanilloid receptor VR1 innervation in vulvodinia. *Eur J Pain* 2004; 8: 129–133.
 37. Yiangou Y, Facer P, Dyer NHC, Chan CLH, Knowles C, Williams NS, Anand P. Vanilloid receptor 1 immunoreactivity in inflamed human bowel. *Lancet* 2001; 357: 1338–1339.

38. Caterina MJ, Schumacher MA, Tominaga M, Rosen TA, Levine JD, Julius D. The capsaicin receptor: a heat-activated ion channel in the pain pathway. *Nature* 1997; 389: 816–824.
39. Maddock AL, Westenfelder C. Urea induces the heat shock response in human neuroblastoma cells. *J Am Soc Nephrol* 1995; 7: 275–282.
40. Liu L, Chen L, Liedtke W, Simon SA. Changes in osmolality sensitize the response to capsaicin in trigeminal sensory neurons. *J Neurophysiol* 2007; 97: 2001–2015.
41. Verbalis JG. How does the brain sense osmolality? *J Am Soc Nephrol* 2007; 18: 3056–3059.
42. Docherty RJ, Yeats JC, Bevan S, Boddeke H. Inhibition of calcineurin inhibits the desensitization of capsaicin-evoked currents in cultured dorsal root ganglion neurones from adult rats. *Pflügers Arch* 1996; 431: 828–837.
43. Bhawe G, Zhu W, Wang H, Brasier DJ, Oxford GS, Gereau RW. Gereau RW IV. c-AMP dependent protein kinase regulates desensitization of the capsaicin receptor (VR1) by direct phosphorylation. *Neuron* 2002; 35: 721–731.
44. Taiwo YO, Bjerknes LK, Goetzl EJ, Levine JD. Mediation of primary afferent peripheral hyperalgesia by the cAMP second messenger system. *Neurosci* 1989; 32: 577–580.
45. Taiwo YO, Levine JD. Further confirmation of the role of adenylyl cyclase and of cAMP-dependent protein kinase in primary afferent hyperalgesia. *Neurosci* 1991; 44: 131–135.
46. Ji R-R, Gereau RW, IV, Malcangio M, Strichartz GR. MAP kinase and pain. *Brain Res Rev* 2009; 60: 135–148.
47. Story GM, Peier AM, Reeve AJ, Eid SR, Mosbacher J, Hricik TR, Earley TJ, Hergarden AC, Andersson DA, Hwang SW, McIntyre P, Jegla T, Bevan S, Patapoutian A. ANKTM1, a TRP-like channel expressed in nociceptive neurons, is activated by Cold Temperatures. *Cell* 2003; 112: 819–829.
48. Okazawa M, Inoue W, Hori A, Hosokawa H, Matsumura K, Kobayashi S. Noxious heat receptors present in cold-sensory cells in rats. *Neurosci Lett* 2004; 359: 33–36.
49. Bennion BJ, Daggett V. The molecular basis for the chemical denaturation of proteins by urea. *Proc Natl Acad Sci U S A* 2003; 100: 5142–5147.
50. Mahoney CA, Arief AI. Uremic encephalopathies: clinical, biochemical, and experimental features. *Am J Kidney Dis* 1982; 2: 324–336.
51. Gropman AL, Summar M, Leonard JV. Neurological implications of urea cycle disorders. *J Inherit Metab Dis* 2007; 30: 865–879.
52. Vonsattel JP, Myers RH, Stevens TJ, Ferrante RJ, Bird ED, Richardson EP Jr. Neuropathological classification of Huntington's disease. *J Neuropathol Exp Neurol* 1985; 44: 559–577.
53. Xu J, Begley P, Church SJ, Patassini S, Hollywood KA, Jüllig M, Curtis MA, Waldvogel HJ, Faull RLM, Unwin RD, Cooper G. Graded perturbations of metabolism in multiple regions of human brain in Alzheimer's disease: snapshot of a pervasive metabolic disorder. *Biochim Biophys Acta* 2016; 1862: 1084–1092.
54. Handley RR, Reid SJ, Brauning R, Maclean P, Mears ER, Fourie I, Patassini S, Cooper GJS, Rudiger SR, McLaughlan CJ, Verma PJ, Gusella JF, MacDonald ME, Waldvogel HJ, Bawden CS, Faull RLM, Snell RG. Brain urea increase is an early Huntington's disease pathogenic event observed in a prodromal transgenic sheep model and HD cases. *Proc Natl Acad Sci U S A* 2017; 114: E11293–E11302.